Preparation of Electronically Conducting Ultra-Thin Polymer Films

Gyoujin Cho

Department of Chemical Engineering, Suncheon National University, 315 Maegok, Suncheon, Chonnam 540-742, Korea

(Received January 21, 1997)

Admicellar polymerization uses adsorbed surfactant aggregates to concentrate monomeric species at the solution–solid interface and to localize the polymer-forming reaction over a surface. The process has been adapted for the deposition of polypyrrole thin films on mica substrates. Amphiphiles adsorb from aqueous solution onto mica substrates and form self-assembled arrays. These arrays have been characterized by atomic force microscopy (AFM). Polypyrrole films prepared by polymerization in the self-assembled arrays (PSAA) were characterized and compared with samples made by polymerization in the absence of self-assembled arrays (surface nucleation, PSN). Images and measurements by AFM indicate that PSAA films over mica surfaces tend to be much smoother than PSN layers at the same condition. The ultra-thin PSAA (130 nm) can be fabricated simply, controlled by changing the ratio between water, surfactant, and pyrrole concentration under ambient conditions. Although thinner, PSAA films have more stable and higher conductivity than the PSN films. The relationship between film morphology and electronic properties has been discussed.

Conducting polymers (CP) are currently being investigated for use as battery electrodes, for corrosion protection, and in biological sensors.[1—4] CP films can be presently prepared either chemically or electrochemically in various media (e.g., an organic solvent,[5] water,[6—8] and confined two-dimensional structures[9]).

The formation of ultra-thin CP films on substrates such as microarray electrodes is an indispensible technique for rapid and clear responses in sensor technologies.[10,11] Although thin films of CP are easily grown electrochemically on conducting surfaces, the formation of uniform thin films on insulating materials, such as mineral oxides, is difficult. In my recent research, amphiphiles have been utilized to construct two-dimensional media on the surface of alumina particles. This method may be applied to produce highly conducting, ultra-thin polypyrrole (PPY) film coatings on insulating materials on an industrial scale.[12]

Since PPY in general have poor mechanical properties, various techniques[13—15] have been applied to improve both their mechanical properties and their electrical conductivities. Among these techniques, the use of both self-assembled arrays (SAA) and ordered, semicrystalline media for the polymerization of pyrrole have been investigated and have proven moderately successful, especially in the fabrication of organic microelectronic devices.

As part of an ongoing project, this paper reports the initial results obtained from the characterization of both the SAAs of hexanoic acid adsorbed on mica, along with the resulting thinly-deposited PPY films, through the use of contact angle measurements, atomic force microscopy (AFM), scanning tunneling microscopy (STM), conductivity measurements, and reflection-absorption IR (RAIR). The measurements described in this work on the characteristic properties of absorbed SAAs (of hexanoic acid) on mica were obtained by applying both the Wilhelmy plate method[16] and AFM. In the Wilhelmy plate method, both the advancing and receding contact angles were calculated from the forces exerted as a given sample is either immersed or withdrawn from a liquid.

The AFM was selected for the measurement of film thickness and the study of morphology, since it can measure the film thickness by scanning at the interface between masked and unmasked sections of a mica plate. Using the PPY film thicknesses obtained by AFM, the temperature dependences of conductivity of the resultant thin PPY films on mica were measured using a four-probe configuration. Additionally, both the PPY surface morphology and structure were investigated using AFM, STM, and RAIR.

Experimental

Materials. Hexanoic acid (99%, Aldrich) was dried over $MgSO_4$ and fractionally distilled from $CaSO_4$. Pyrrole (98%, Aldrich) was purified by passage through a short column of basic alumina, activity grade I (Sigma). Reagent grade ammonium peroxodisulfate (Mallinckrodt) and sodium chloride (Baker) were used without further purification. Doubly-distilled water was used in all systems. Muscovite mica disks were purchased from Asheville–Schoonmaker Mica Co. and used only after peeling off the contaminated top surface layers.

Characterization of Adsorbed SAA of Hexanoic Acid on Mica Using the Wilhelmy Plate Method. A Cahn Model 29 microbalance and a stepper moter (used to move a supporting platform), monitored the immiscible liquid samples using IBM PC/XT. The mica on glass (as a standard sample) handing from the balance was then immersed in and removed from the liquids in a continuous motion so that immersion–immersion cycles or "wetting cycles" could be obtained. A wetting cycle run consisted of moving the interfaces 25.4 mm up and then 25.4 mm down at a standard speed of 0.127 mm s^{-1}. During this movement, 720 data values were recorded by the microcomputer.

Glass microscope cover slides were used in this study as a standard. The glass slides were cleaned by first soaking in chromic acid, rinsing with distilled water, rinsing again with Baker reagent grade acetone, and then flamed. Deionized and doubly-distilled water was used as the liquid. The surface tension for the water liquid as measured with glass slide and the Wilhelmy device was 76.8 dyn cm^{-1}. The freshly-cleaned bare mica plates were then prepared by simply peeling off the top layer. The hexanoic acid-adsorbed micas were prepared by simply immersing the mica plate into hexanoic acid solutions adjusted to pH levels of 2 and 6 using 6 M HCl solution (1 M = 1 mol dm^{-3}) for 12 h and then drying it in a desiccator for 2 d. The dried (hexanoic acid adsorbed) mica was used without further treatments.

Polymerization of Pyrrole on Mica Surfaces. Freshly-peeled mica disks (1.5 cm diameter) were placed in 4 dram vials and covered with 5 mL of one of the following three monomer solutions: 20 mM pyrrole; 20 mM pyrrole and 15 mM hexanoic acid; 20 mM pyrrole, 15 mM hexanoic acid, and 1.5 M salt. The vials were placed in a bath at 30 °C. After 1 h, an equimolar amount of ammonium peroxodisulfate (based on the pyrrole) was added as a concentrated solution. After 4 h, the plates were rinsed with distilled water and dried in a desiccator for 1 d. For thickness measurements (of the deposited film on the mica substrate), the same experimental procedures were used, except for masking one part of the plates using Teflon® tape. After surface polymerization, clear interfaces between the bare mica and PPY film deposited mica parts were obtained by simply removing the Teflon® tape. These partially-deposited mica plates were used in AFM, STM, conductivity, and RAIR measurements without further modification.

Conductivity Measurements. The PPY-treated mica was cut into 0.5×1.5 cm size rectangles which were mounted on four nickel wires with silver paste. The nickel wires had been sealed into a rubber stopper with a ground glass sleeve which could be fitted into a glass tube equipped with Teflon® stopcocks for purging and evacuation. A Teflon®-covered thermocouple was fitted through a septum and attached to a platinum wire near the sample to monitor temperature. All measurements were carried under an argon atmosphere. Voltage measurements were carried out using a Kiethley 610C electrometer and Kiethley 175 multimeter, respectively. Constant currents were obtained using the Kiethley 610C or Lakeshore Crygenics 120 current source. Temperature was controlled by use of a liquid nitrogen bath. The conductivity (s/s cm^{-1}) was calculated using the expression

$$s = (i/V)(l/dw), \tag{1}$$

where i is the current applied, V is the voltage measured across the inner two electrodes, d is the sample thickness, l is the spacing between the inner two electrodes, and w is the width of the sample.

Morphology Characterization using AFM, and STM. The AFM and STM measurements were carried out using a Multimode Scanning Force Microscope from Digital Instruments. The AFM images were taken in "constant force" mode and the STM was done in "constant current" mode. All the samples were scanned in air at room temperature. We used the standard silicon nitride tips for AFM and Pt–Ir tips for STM.

To conform reproducibilities of the superstructure images, we also used the sharpest etched silicon tips (ESP) available to image those chevron features and to make sure to minimize any tip artifacts. The ESP tip can scan the object side angle correctly up to 80° relative to the horizontal plane. The face angles of those superstructures with respect to the substrate fall between 40° to 60°, well below the tip capacity. All the tips were purchased from Digital Instruments. The film thickness was obtained through the cross-sectional profile analysis on the image.

Morphology Characterization using RAIR. IR spectra of the deposited films on mica were taken by reflection of the incident beam with a Perkin–Elmer 1800 FTIR equipped both with a narrow band mercury–cadmium–telluride liquid nitrogen-cooled detector, a 1 mm^2 active area and a cutoff at about 700 cm^{-1}. (Spectra were taken at 2 cm^{-1} resolution). Interferograms were collected in double precision and Fourier-transformed with triangular apodization. Reference spectra were obtained from an evaporated gold-covered slide glass. Nitrogen purge gas was passed through molecular sieves and a charcoal filter.

Results and Discussion

The previous paper describes the mechanism proposed in our laboratory for hexanoic acid adsorption at water–alumina interfaces.[12,17] This mechanism is not only strongly pH-dependent, but also represents a transition from a patch-growth type adsorption to a simple Langmuir type during increases in the pH level from values of 2 to 6.[17] It is thus postulated at this point that the same mechanism may in turn also be applicable to that of the adsorption of hexanoic acid on mica–water interfaces. This assumption implies that the formation of the patch-growth type SAAs of hexanoic acid (at pH levels of 2) and Langmuir-type SAAs of hexanoic acid (at pH levels of 6), respectively, may be expected. Therefore, application of both the Wilhelmy plate method for determining the contact angles and AFM should allow for characterization of adsorbed SAAs of hexanoic acid on mica substrates.

Characterization of Adsorbed SAAs on Mica by the Wilhelmy Plate Method. Typical wetting cycles were obtained by the Wilhelmy plate method and contact angles were calculated using Eq. 2;

$$F = Pg\cos q - B, \tag{2}$$

where F is the force on a plate partially submersed in liquid, P is the plate perimeter, g is the surface tension of the solvent, q is the contact angle, and B is the buoyancy of that portion of the plate below the overall surface.

Both the advancing and receding contact angles for bare mica as well as hexanoic acid-adsorbed mica at (pH levels of 2 and 6) were calculated using the value for the water surface tension (77.8 dyn cm^{-1}) obtained in this work with the previously-described apparatus with glass slides (the resulting contact angles are listed in Table 1). From the information obtained about the advancing contact angles, it is clear that, although hexanoic acid adsorbed more effectively on mica at pH levels of 2 than at pH levels of 6, these advancing contact angles are actually smaller than those obtained for common hydrophobic surfaces[18] (e.g., an alkanethiol-adsorbed Au surface yields an advancing contact angle of 110°).

Although the adsorption of hexanoic acid on mica surfaces has been proven by both contact angle measurements as well as with the wetting cycles, uncertainties remain concerning the surface structures of adsorbed SAAs of hexanoic acid on mica. The use of AFM to characterize the structure of the adsorbed SAA hexanoic acid may therefore prove useful.

Table 1. Advancing and Receding Angles for Bare Mica and Modified Mica

	Bare mica	Hexanoic acid adsorbed mica at pH 2	Hexanoic acid adsorbed mica at pH 6
Advancing contact angle	0°	50°	20°
Receding contact angle	0°	0°	0°

Characterization of the Adsorbed SAA, on the Mica Surface by AFM. For this work, it is more practical to investigate the structure of adsorbed SAA on mica at a pH level of 2 due to the greater amount of hexanoic acid adsorbed on the mica surface (as expected from the wetting measurements reported). This procedure is described in detail at the experimental section.

First, the fresh bare mica surface was scanned to reveal the image of the bare mica surface (as seen in Fig. 1). The cross section of the bare mica image (obtained in this work) indicates that the bare mica surface possesses an Å-range roughness (i.e., a surface root-mean-square (rms) roughness of 2 Å).

The hexanoic acid-adsorbed mica sample from a pH level of 2 yields AFM images in Fig. 2 quite different from those of bare mica surface. The images of Fig. 2 reveal that ordered features are not observed, but many island-type shapes are easily discernible.

Such disordered features are not surprising, since it has been previously reported that adsorbed amphiphilic molecules possessing short alkyl chains (typically less 8 carbon units long) usually result in disordered structures (e.g., a two-dimensional liquid); this is due in part to their low melting points (less than that of room temperature) on a given surface.[19] The bright spots observed in Fig. 2 may be taken to represent patch-like, surface structures consisting of agglomerations of adsorbed hexanoic acid on mica and formed islands which is not irreversible. The previously reported AFM images of physically adsorbed amphiphilic molecules on mica were island-type as well.[20] The geometrical surface coverage of SAA islands is approximately 50%, with the size of islands varying in radius from 0.1 μm to a few nm. For mica treated at the pH level of 6, hexanoic acid surface structures were not observed, confirming the earlier wetting studies which suggested low surface coverage.

The AFM results obtained for this work are thus shown to be consistent with the results of wetting experiments, i.e., the surface is not completely covered by adsorbed hexanoic acid. The preliminary results represented in this work therefore provide a reasonable basis to postulate that the adsorbed hexanoic acid actually exists in a 2-dimensional liquid state on the mica surface.

Thickness Measurements of Deposited PPY Films. To investigate the influence of SAA on thinly-deposited PPY films, it is interesting to note the change in thickness between the PPY films deposited on bare mica and PPY

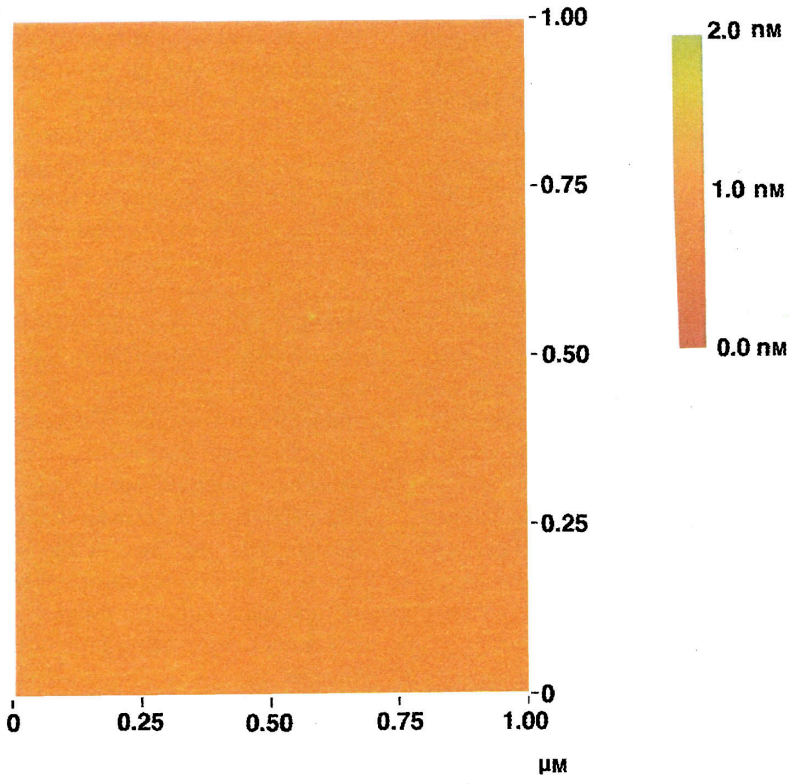

Fig. 1. AFM image for the bare mica surface.

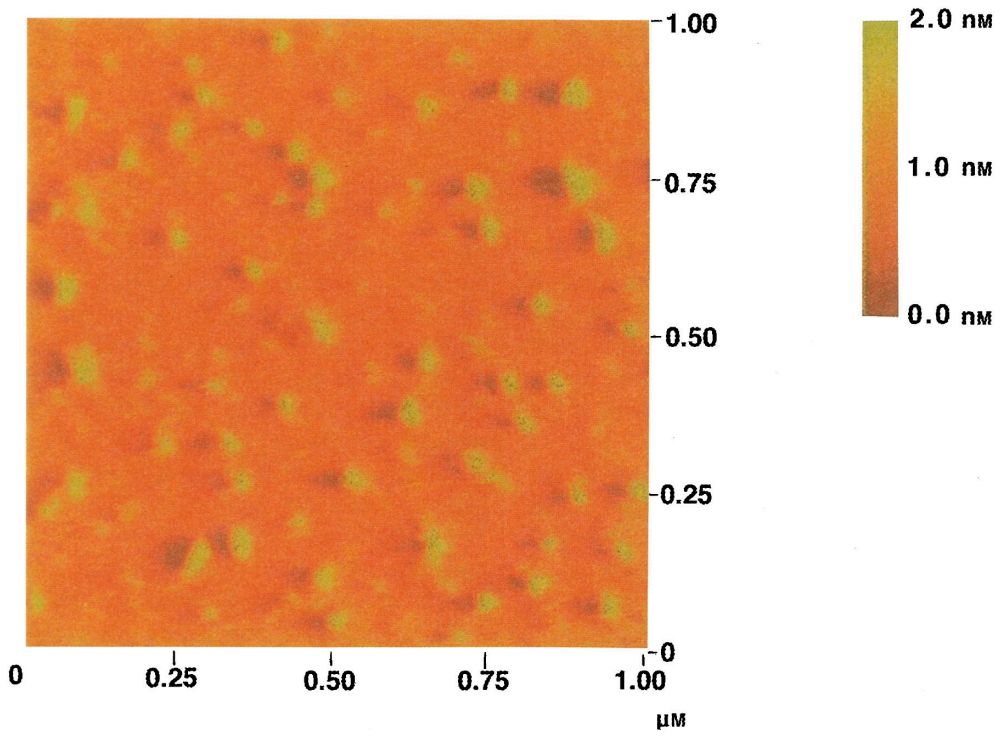

Fig. 2. AFM image for the hexanoic acid adsorbed on mica surface at the pH level of 2.

films deposited on mica modified by the adsorption of amphiphilic molecules. Three samples (i.e., consisting of water–mica (PD1), water/hexanoic acid–mica (PD2), and water/salt/hexanoic acid–mica (PD3) systems) were prepared followed experimental procedures.

From the cross-sectional slices of AFM images (Fig. 3), the film thickness and surface roughness for each sample may easily be measured (with the thicknesses obtained for the PPY films deposited presented in Table 2). From the PD3 (water/salt/hexanoic acid–mica) systems, deposited PPY films roughly 130 nm in thickness may easily be detected by the naked eye. In addition, the PD2 (water/hexanoic acid–mica) and PD1 (water–mica) systems, reveal PPY films roughly 150 nm (Fig. 3) and 170 nm in thickness, respectively, which can also be seen by the naked eye. It should be noted that all of these determined thicknesses are reproducible except for the PD1 system.

The mechanism of surface polymerization of pyrrole at the interfaces of the PD2, and PD3 systems may be speculated upon to be a lateral growth of polymer chains along the interface between adsorbed SAA on mica and water. The vertical growth by oligomer precipitation (as a nucleation site) on the surface may then be postulated as a second mechanism to account for pyrrole polymerization within the PD1 system. Although many factors can affect the thickness of the deposited PPY films, the different film thickness of the deposited PPY films from PD1, PD2, and PD3 my originate from those two different mechanisms.

Table 2. Thickness of PPY Film Deposited on Mica under PD1, PD2, and PD3 Conditions

Samples	PD1	PD2	PD3
Thickness/nm	170	150	130

Electrical Properties. Differences in both the chemical makeup and structure of conductive organic systems are often revealed through their electrical properties.[23] For this work, the temperature-dependent conductivity for each PPY-deposited mica sample was quantified using four probe measurements under an argon atmosphere. The results, obtained over a wide temperature range (i.e., 143 to 333 K), are given in Fig. 4. Although all samples reported herein show a positive temperature coefficient for their respective conductivities, the temperature dependence of the conductivity is in fact nearly exponential and extremely weak. Figure 4 shows that, under the given conditions, all PPY-deposited mica plates studied display activation energies (slopes calculated from the data in Fig. 4 using linear regression) of between 95 and 38 meV, with conductivities ranging from 35 to 9.3×10^{-2} s cm^{-1} at 20 °C (i.e., they comprise both semiconductors and metals). The sample displaying the greatest conductivity was the PPY-deposited on mica plate in the PD3 (water/hexanoic acid/salt–mica) system.

The above-mentioned electrical measurements are therefore primarily presented in this work to show that the PPY films deposited on the mica are well-aggregated (i.e., without any major domain barriers). This is suggested by the conductivities being largely unaffected by temperature (since, if there were domain boundaries, the conductivities of each sample would be strongly influenced by temperature changes). It was therefore clear that further characterization of the surface morphology of PPY films deposited on mica would help us to understand not only the observed temper-

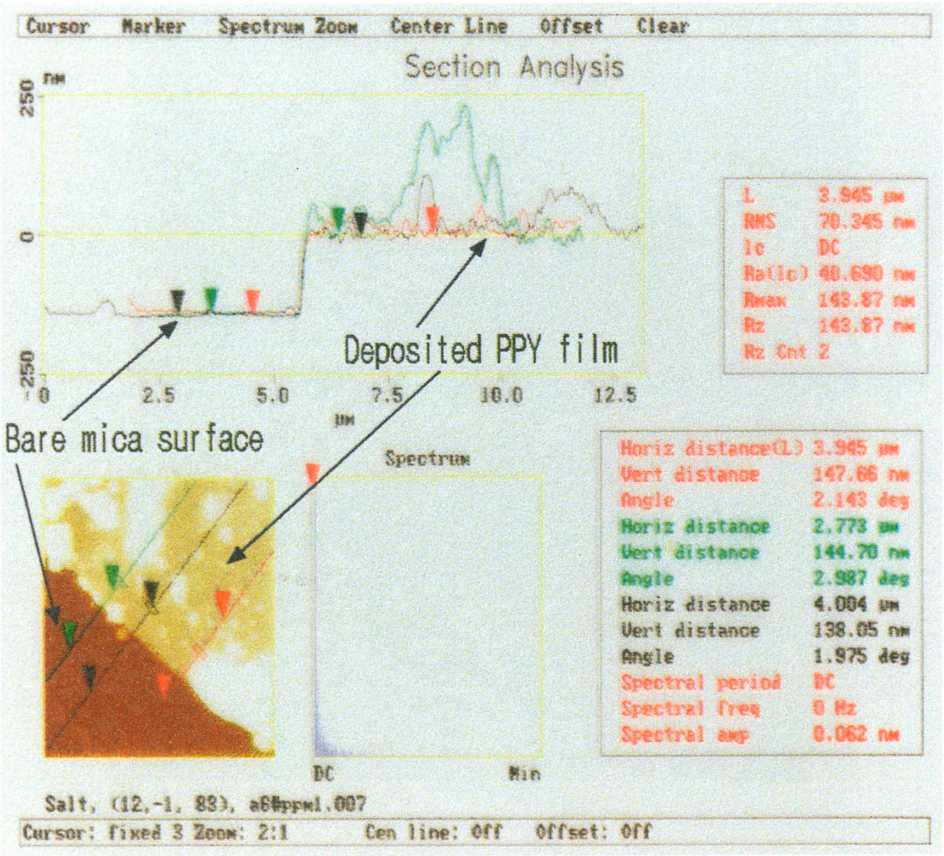

Fig. 3. AFM topograph and cross-sectional analysis of PPY deposited mica sample (PD2) within the interface region.

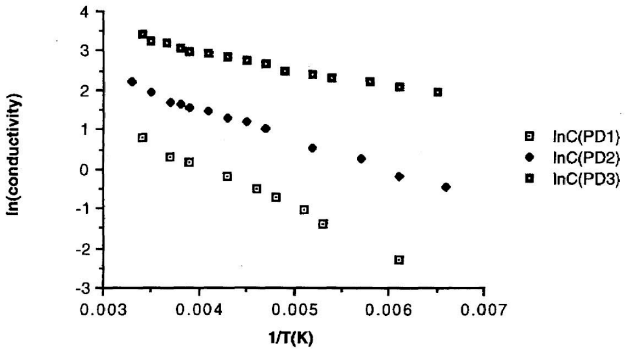

Fig. 4. Temperature dependant conductivities measurements at various systems: PD1, PD2, and PD3.

ature-dependent conductivities, but also the overall features of the PPY-deposition mechanism on mica.

Surface Characterization by AFM, STM, and RAIR. The morphology of the deposited PPY films on mica was initially studied via optical microscopy, where the macroscopic features of the PPY film surfaces were observed. From these nonpolarized optical microscopy results (see Fig. 5) which were roughly within the 200×200 μm range, many chevron-like superstructures appear to be well-scattered over the entire PPY-deposited mica surface prepared under the PD1 (water–mica), PD2 (water/hexanoic acid–mica), and PD3 (water/hexanoic acid/salt–mica) conditions.

Before taking into account additional characterization of these superstructures within the PPY films deposited on the mica surfaces, precautionary measurements using AFM were first undertaken to confirm that such superstructures are reproducible and not merely due to contamination by salt or other impurities. These measurements confirmed that these superstructures indeed did occur as a result of the PPY using STM (see Fig. 6).

Further characterization of the morphology of the PPY films deposited on mica were undertaken using AFM. In the smooth region, AFM images of PPY films deposited on mica are presented in Fig. 7. In the rough region, many chevron-like and pyramidal superstructures were observed (see Fig. 8). All samples prepared under PD1 (water–mica), PD2 (water/hexanoic acid–mica), and PD3 (water/hexanoic acid/salt–mica) conditions, showed the surface images similar to those shown in Fig. 7 in the smooth region.

Reflection absorption IR spectra (RAIR) were taken for the each sample (e.g., those with and without superstructures). The reproducibility of these spectra was checked by data obtained from two separate experiments performed at each polymerization condition on the mica surface.

The significant features of the spectra of the deposited films (containing superstructures on the mica surface) are a strong band at 1100 cm^{-1}, as well as an absence of an N–H stretching band near 3300 cm^{-1} (it is well-known that the N–H stretching band often disappears from the spectral analysis due to oxidation.[24] In addition, although the correct assignment for the characteristic strong band at 1100 cm^{-1} is

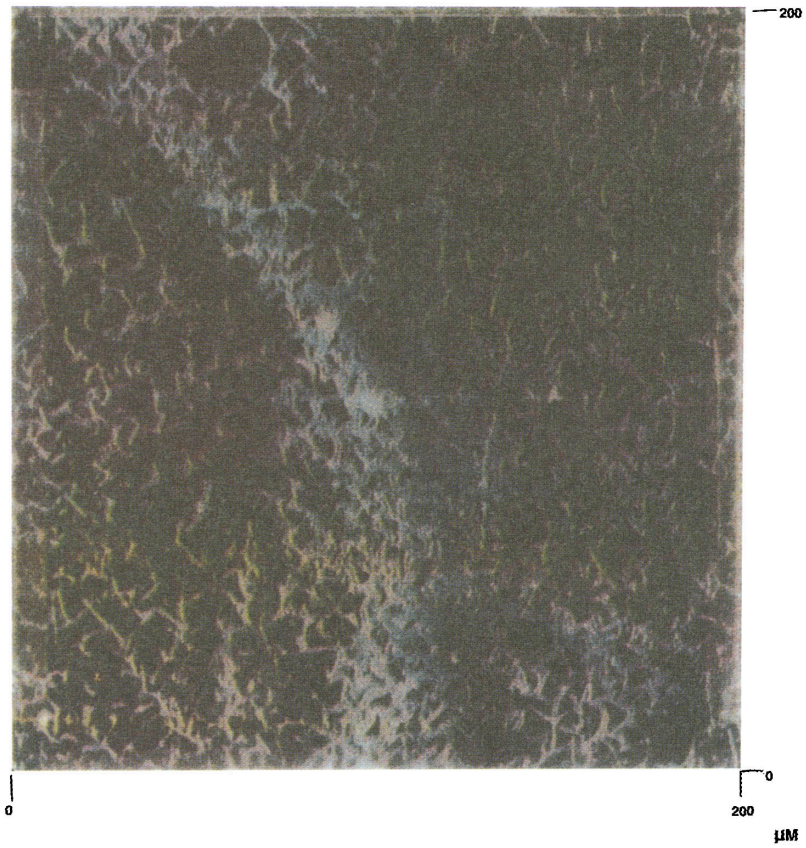

Fig. 5. Optical microscope image (200×200 μm) for the PPY deposited mica surface sample (PD2).

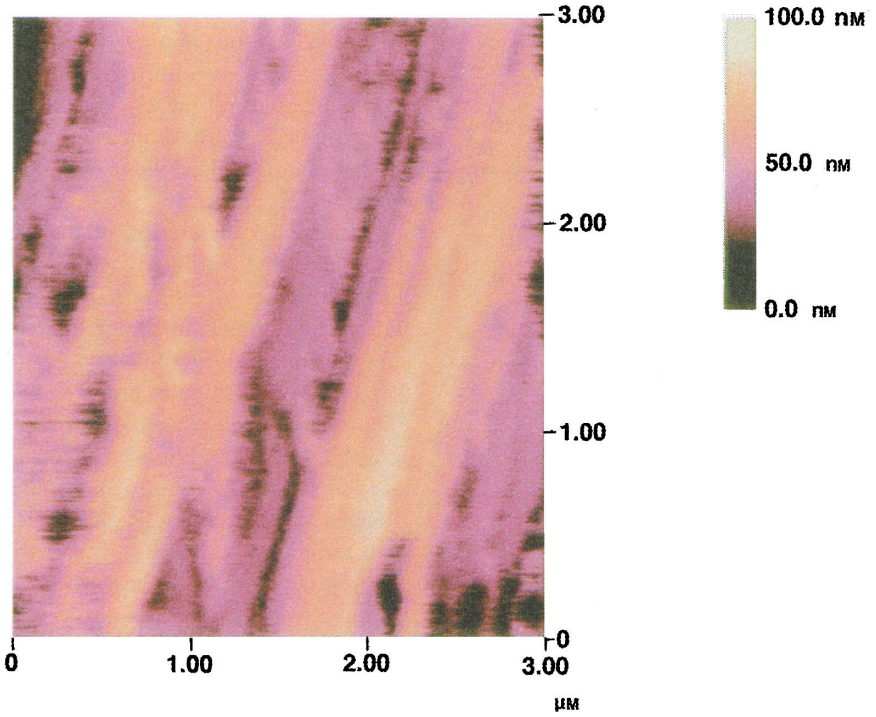

Fig. 6. STM image (3×3 μm) for the PPY deposited mica sample at the superstructure region.

unknown at this point (due to a lack of literature information), it is hereby proposed that (based on the comparisons with the reported Raman spectra of films prepared on a Pt electrode[23]) the strong peak at 1100 cm^{-1} may be assigned to the C–H in-plane bend. Unfortunately, the reason for the other peaks being suppressed cannot currently be explained, especially

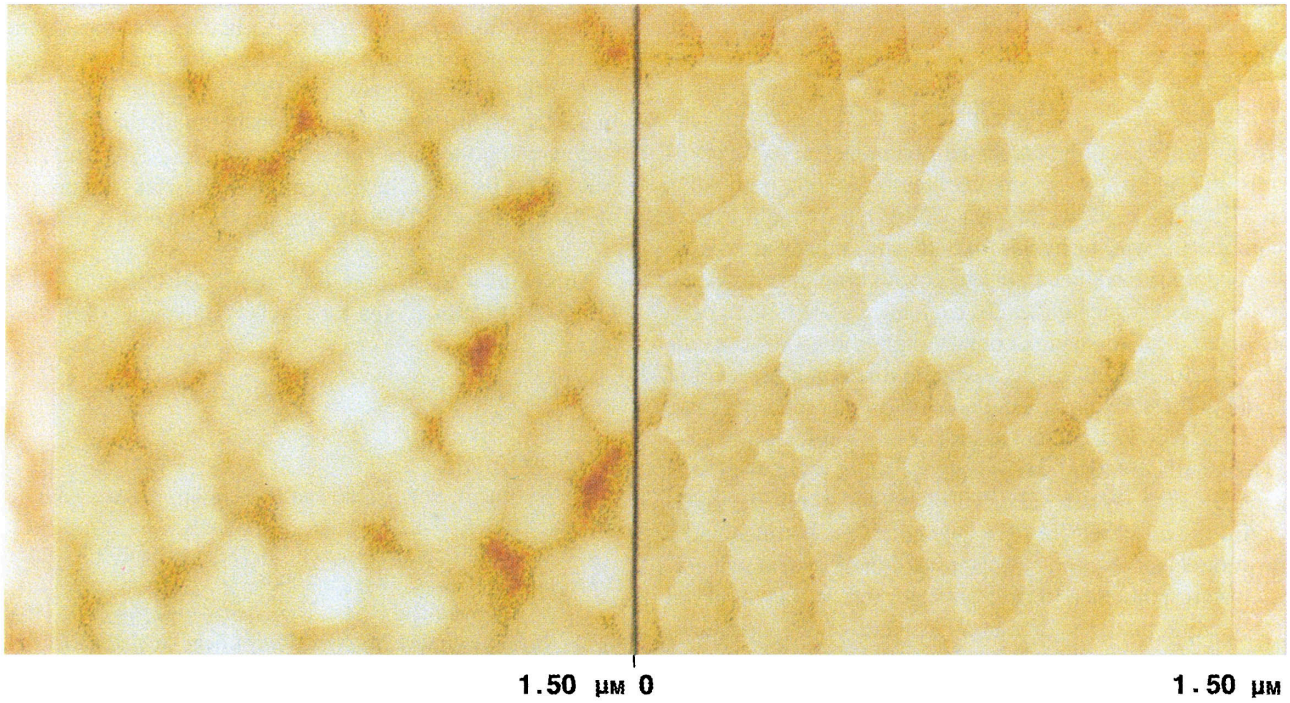

Fig. 7. AFM image for the PPY deposited mica sample (PD3) in the smooth region.

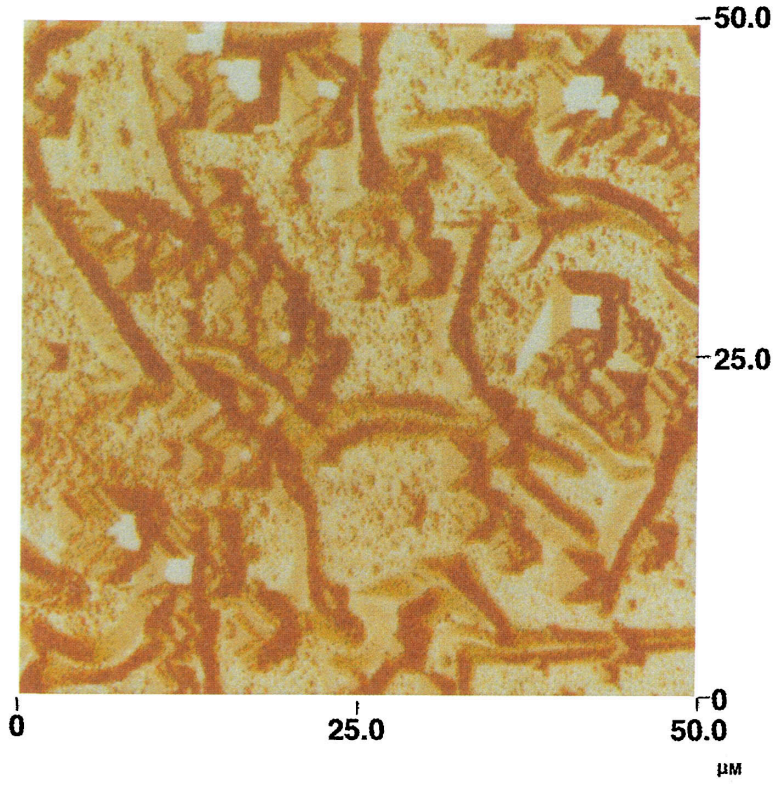

Fig. 8. AFM image for the PPY deposited mica (PD3) in the rough region.

for the O=C/C–C stretch bands (which are usually observed as the strongest bands near 1550 cm^{-1}).

The RAIR spectra for the PPY films (without superstructures) coated on the mica surface after initially forming the PPY film at water–air interface show the same features as normal PPY spectrum. The observed RAIR spectra for samples without any superstructures are completely different from those observed for those samples containing the crystalline superstructures. The characteristic strong band at at 1100 cm^{-1} has disappeared in the spectra of both the deposited and transferred films without the superstructures on the mica substrate. It is therefore not very difficult to postulate that

the appearance of the strong band at 1100 cm^{-1} may be due to the superstructures.

Conclusion

Adsorbed SAA of hexanoic acid on mica (prepared at pH levels of 2 and 6) have been characterized using both AFM and Wilhelmy plate techniques. With the Wilhelmy plate technique, the wetting cycles for both bare and hexanoic acid-adsorbed mica have been presented with both the advancing and receding contact angles for each mica plate having been calculated. The advancing contact angle showed 0° for bare mica, 50° for hexanoic acid-adsorbed mica (at a pH level of 2), and 20° for hexanoic acid adsorbed mica (at a pH level of 6). The receding contact angle for all samples was 0°.

The results obtained from these wetting cycles were well matched to the results indicated by AFM. From the AFM images, the adsorbed SAA of hexanoic acid on mica had a near-monolayer thickness (2 nm), with their structures bearing close resemblence to patch-like shapes. It was observed in this work that only about 50 percent of the mica surface was covered by these patch-like adsorbed hexanoic acid structures to yield the hydrophobic properties of the mica surface.

The surface polymerization of PPY was carried out under three different conditions (e.g., water–mica (PD1), water/hexanoic acid–mica (PD2), and water/salt/hexanoic acid–mica (PD3) conditions). The deposited films resulting from the above five conditions showed various thicknesses ranging from 130 to 170 nm. The film thickness were easily determined using an AFM profilometer.

Based on these determined thicknesses, the temperature-dependent electronic conductivities of each sample were also examined. The highest-obtained conductivity at 20°C was 35 s cm^{-1} (with a 134 nm film thickness) for the PPY-deposited film on the mica surface (under the PD3 condition). The calculated activation energies were very low (i.e., 30 to 90 meV) for all samples reported. From these results, it may be expected that the deposited films on mica are both very dense and well-connected. Those films were subsequently investigated by characterization of the morphology of the PPY-deposited films on mica using both the AFM and STM. In addition to the well-packed granular sharp of the deposited-film AFM images (as seen in Fig. 7), the most interesting observation among these images was that of unexpected superstructures bearing crystalline shapes. These crystalline shapes revealed in the superstructure images have been confirmed not to be artifacts of the AFM tip, since those images also showed up using STM analysis. Moreover, the STM images (Fig. 6) obtained were shown to be quite similar to those of known crystalline STM images.[24)]

By careful considerations based on the results obtained in this work, it may be speculated that the PPY growth direction (lateral or vertical) is controlled by the adsorbed SAA hexanoic acid on the mica substrate. While the PPY film may grow effectively along the pyrrole-concentrated interface (with the adsorbed SAA on the mica), it may also epitaxially grow along the lattice on bare mica without the adsorbed SAA. The aforementioned superstructures may therefore be due to the epitaxial growth of PPY along the mica lattice. In RAIR spectra, those films deposited with the PPY superstructures on the mica surface reveal a characteristic strong band at 1100 cm^{-1}. Such a band, however, was not observed on the deposited PPY films without the superstructures.

This work was supported by the NON DIRECTED RESEARCH FUND, Korea Research Foundation, 1996 (04-E-0060).

References

1) S. Panero, P. Prosperi, and B. Scrasuti, *Electrochim. Acta*, **32**, 1965 (1987).
2) C. A. Ferriera, S. Aeiyach, M. Delamar, and P. C. Lacaze, *J. Electroanal. Chem.*, **284**, 35 (1990).
3) N. C. Foulds and C. R. Lowe, *Anal. Chem.*, **60**, 2473 (1988).
4) F. Mizutani and M. Asai, *Bull. Chem. Soc. Jpn.*, **61**, 4458 (1988).
5) A. F. Diaz, J. I. Casillo, J. A. Lognan, and W.-Y. Lee, *J. Electroanal. Chem.*, **129**, 115 (1981).
6) T. F. Otero, R. Tejuda, and A. S. Eloda, *Polymer*, **28**, 651 (1987).
7) L. F. Warren and D. P. Anderson, *J. Electrochem. Soc.*, **134**, 101 (1987).
8) F. A. Valk, B. C. Schuermans, and E. Barendrecht, *Electrochim. Acta*, **35**, 367 (1990).
9) G. M. Whitesides and P. E. Laibinis, *Langmuir*, **6**, 87 (1990), and references therein.
10) T. Matsue, M. Nishizawa, T. Sawaguchi, and I. Uchida, *J. Chem. Soc., Chem. Commun.*, **1991**, 1092.
11) M. Nishizawa, T. Matsue, and I. Uchida, *Sensor Actuators*, **B13**, 53 (1993).
12) G. Cho, D. T. Glatzhofer, and B. M. Fung, submitted for the publication in *Langmuir*.
13) K. Hong, R. B. Rosner, and M. F. Rubner, *Chem. Mater.*, **2**, 82 (1990).
14) D. M. Collard and M. A. Fox, *J. Am. Chem. Soc.*, **113**, 9414 (1991).
15) K. Kawai, N. Mihara, S. Kuwabata, and H. Yoneyama, *J. Electrochem. Soc.*, **137**, 1793 (1990).
16) Y. K. Kamath, C. J. Dansizer, and H. D. Weigman, *J. Colloid Interface Sci.*, **102**, 164 (1984).
17) G. Cho, Ph. D. Dissertation, University of Oklahoma, Norman, OK (1995).
18) M. D. Wilson and G. M. Whitesides, *J. Am. Chem. Soc.*, **110**, 8718 (1988).
19) K. Ohtake, N. Mino, and K. Ogawa, *Langmuir*, **8**, 2081 (1992).
20) B. G. Sharma, S. Basu, and M. M. Sharma, *Langmuir*, **12**, 6506 (1996).
21) A. J. Epstein, in "Handbook of Conductive Polymers," ed by T. A. Skothein, Marcel Dekker, New York (1986).
22) R. G. Davidson and T. G. Turnet, *Synth. Met.*, **72**, 121 (1995).
23) K. M. Cheung, D. Bloor, and G. C. Stevens, *Polymer*, **29**, 1709 (1988).
24) J. Li and E. Wang, *Synth. Met.*, **66**, 67 (1994).